Phenomenon of Instantaneous Work Hardening Characteristics of Sintered Cold Deformed Cu Alloy Preforms

A. Rajeshkannan[1, a], S. Narayan[2,b]

[1]Senior Lecturer, Mechanical Engineering, School of Engineering & Physics, Faculty of Science, Technology & Environment, The University of the South Pacific, Laucala Campus, Suva, Fiji, Mobile no. +679 8369513

[2]Assistant Lecturer, Mechanical Engineering, School of Engineering & Physics, Faculty of Science, Technology & Environment, The University of the South Pacific, Laucala Campus, Suva, Fiji

[a]ananthanarayanan_r@usp.ac.fj, [b]narayan_s@usp.ac.fj

Keywords: Instantaneous hardening – strain & density; Instantaneous strength coefficient – strain & density; Aspect ratios.

Abstract. Work hardening behavior is an important phenomenon especially when a material is subjected to cold work. The two important parameters that expose this study are strain hardening exponent, n, and strength coefficient, K, according to ludwik equation, $\sigma = K\varepsilon^n$. In addition to strain as influencing factor for work hardening behavior, the attained density during deformation is also considered in the present investigation; a rational approach and its characteristic evaluation has been proposed. Thus a copper alloy preforms of three different aspect ratios prepared using conventional powder metallurgy method and a secondary deformation such as cold deformation were carried out till maximum density or fracture appears at the outer surface of deforming preforms. The dimensional and density measurements were carried out carefully and the same is utilized to explain the instantaneous work hardening behavior with respect to induced strain and attained density.

Introduction

The powder metallurgy (P/M) route is an eco-friendly and literally produces no scrap that means all the initial material taken can be converted into product without any wastage. Nevertheless, the product produced by P/M route posses less strength due to weak spots like porosity and cannot be used for high strength applications [1]. Therefore, it is necessary to improve its strength, which is dependent on the processes employed [2]. It is also important to note apart from selected composition there are other parameters which also influence such as product geometry and working media [3]. A secondary deformation processes such as pressing or repressing, powder extrusion, powder rolling and infiltration can be used to eliminate the porosity and subsequently increased density of the parts, which in turn improve the mechanical properties [4].

Strain hardening is important in forming operations since it controls the amount of uniform plastic strain that the material would experience during cold forging before crack appears at the free surface. In powder preform forging the rate of increasing stress values with respect to strain values is higher in comparison to conventional materials of the same composition under identical testing conditions. This is due to the continuous closure of pores present in the P/M material which in turn increases the load bearing cross sectional area and so the further deformation would require greater stress resulting in work hardening behavior [5]. Many researchers [2,6,7] have been reported that during cold upsetting of porous materials, the total work hardening is the result of combined effect of induced strain and densification. It is shown [6,8] that apart from usual strain hardening, porous materials experience both geometric and matrix work hardening, where the matrix work hardening is dominant for relative density of 0.9 and higher in Aluminium matrix studied by the authors. Further, for lower initial preform density value, the geometrical work hardening is dominant. It is interesting that without the need of knowing stress-strain rate, determination of the value of strain

hardening exponent has been reported elsewhere [9] using double compression test. According to Baskaran and Narayanasamy [8] and Kumar et al. [10] the value for strain hardening exponent, strength coefficient and formability stress index varies significantly with varying preform geometries, working media and particle size under different stress state conditions during cold upset forging.

Thus, the present investigation evaluates the instantaneous work hardening behaviour of sintered and cold deformed Cu-7%Al-1.8%Si preforms with the influence of three different aspect ratios against induced strain and attained density. An empirical relationship has been obtained for instantaneous strength coefficient and hardening exponent with respect to both strain and density from which matrix and geometric work hardening has been rationalized respectively.

Experimental Details

Electrolytic copper powder (Cu) of -150 µm, atomized aluminium powder (Al) and silicon powder (Si) of - 37 µm size were used in the present investigation. The required amount of powders corresponding to C64200 that is Cu-7%Al-1.8%Si was taken in a stainless steel pot with the powder mixed to porcelain balls (10 mm – 15 mm diameter) with a ratio of 1:1 by weight and was blended for 18 hours to obtain a homogenous mix. Green compacts of 28 mm diameter with 12 mm, 18 mm and 29 mm of height were prepared. The powder blend was compacted on a 0.6 MN hydraulic press using a suitable die, a punch and a bottom insert in the pressure range of 280 ± 10 MPa to obtain an initial theoretical density of 0.80 ± 0.01. These green compacts were thoroughly coated on all surfaces with indigenously developed ceramic coating in order to protect them against oxidation during sintering. These ceramic coated compacts were heated in the electric muffle furnace with temperature of 810°C ± 10°C. At this temperature the compacts were sintered for 100 minutes followed by furnace cooling. These preforms were machined such that to obtain height-to-diameter or aspect ratio of 0.4, 0.6 and 1.0 followed by cold upset forging between a flat die-set in the incremental loading step of 0.02 MN using 0.6 MN capacity hydraulic press. The preforms were deformed under dry friction condition. The deformation process was stopped once a visible crack appeared at the free surface. Dimensional measurements such as deformed height, deformed diameters (including bulged and contact) were carried out after every step of deformation using digital vernier caliper and the density measurements being carried out using the Archimedes principle.

Theoretical Analysis

Work hardening is the consequence of a material subjected to plastic deformation below its recrystallization temperature, so an empirical relationship can be obtained to establish its flow behavior by constructing a plot between flow stress and true strain in log-log scale (refer Fig. 1). Where flow stress, σ_z, and true strain, ε_z, can be determined as following:

$$\sigma_z = \frac{Incremental\ load,\ L_i}{Instantaneous\ area\ of\ cross\ section,\ A_i}. \tag{1}$$

$$\varepsilon_z = ln\left(\frac{h_0}{h_f}\right). \tag{2}$$

where, h_0 and h_f, respectively initial height and deformed height of the preform. However *Eq. 1 & Eq. 2 express the relationship in uniaxial, to make this study more meaningful, a triaxial state of stresses and strains would be considered*. As explained elsewhere [3] the effective stress, σ_{eff}, and effective strain, ε_{eff}, for triaxial stress state can be given as following with the assumption that radial stress, σ_r, is equal to hoop stress, σ_θ, as preform is of cylindrical shape.

$$\sigma_{eff} = \left(\frac{\sigma_z^2+2\sigma_\theta^2-R^2(\sigma_\theta^2+2\sigma_z\sigma_\theta)}{2R^2-1}\right)^{0.5}. \quad (3)$$

$$\varepsilon_{eff} = \left[\left(\frac{4}{3(2+R)}\right)((\varepsilon_\theta-\varepsilon_z)^2)+\left(\frac{\varepsilon_z+2\varepsilon_\theta^2}{3}\right)(1-R^2)\right]^{0.5}. \quad (4)$$

where, ε_θ, hoop strain and R is the relative density, that is the ratio between deformed density to theoretical density. In Eq. 3 and Eq. 4, the theoretical relationship for parameters such as hoop stress and hoop strain can be referred elsewhere [6]. It has been reported by Rajeshkannan *et al.* [11] that the empirical relationship that obtained between flow stress and true strain from log-log plot (Fig. 1) as $\sigma = K\varepsilon^n$, can be modified to determine instantaneous strength coefficient, K_i, and instantaneous hardening exponent, n_i, due to induced strain can be given as follows,

$$K_i = \frac{\sigma_m-\sigma_{m-1}}{\varepsilon_m^n-\varepsilon_{m-1}^n}. \quad (5)$$

$$n_i = \frac{ln\left(\frac{\sigma_m}{\sigma_{m-1}}\right)}{ln\left(\frac{\varepsilon_m}{\varepsilon_{m-1}}\right)}. \quad (6)$$

where, σ_m & σ_{m-1} and ε_m & $\varepsilon_{m-1}$are respectively consecutive effective stresses and consecutive effective strains. A very similar approach has been adopted to exhibit a relationship between flow stresses and attained density. For which a semi log plot can be drawn (refer Fig. 2), as the increment of density falls in a short span, so density cannot be taken into log scale. On the other hand the semi-log plot also reveals the original mechanism, which is discussed under *results and discussion* section. Its empirical relationship found to follow as,

$$\sigma = Ce^{bR}. \quad (7)$$

where, C, refers to strength coefficient due to density enhancement and b, refers to hardening exponent due to density attained. The incremental load applied can be specified as 1, 2, 3, … , $(i-1)$ and i. This can be substituted in Eq. 7 and simplified to yield relationship for instantaneous strength coefficient, C_i, and instantaneous hardening exponent, b_i due to density can be written as,

$$b_i = \frac{ln(\sigma_i/\sigma_{i-1})}{R_i-R_{i-1}}. \quad (8)$$

$$c_i = \frac{\sigma_i-\sigma_{i-1}}{e^{bR_i}-e^{bR_{i-1}}}. \quad (9)$$

Results and Discussion

Sintered Cu-7%Al-1.8%Si preforms were subjected to secondary operations to enhance its density subsequently to enhance its mechanical strengthening. The load has been applied in an incremental step, and so its plastic deformation, therefore it is expected that cold deformation of bulk preform interlocks the movement of dislocation to enhance the resistance to deformation; on the other hand further application of load would enhance the density of the preform. Meaning thereby to deform further the same specimen would require higher load, this behavior can be well established by constructing a plot between flow stress and induced strain and attained density in log-log scale and semi log scale, which is shown in Fig. 1 and Fig. 2 respectively.

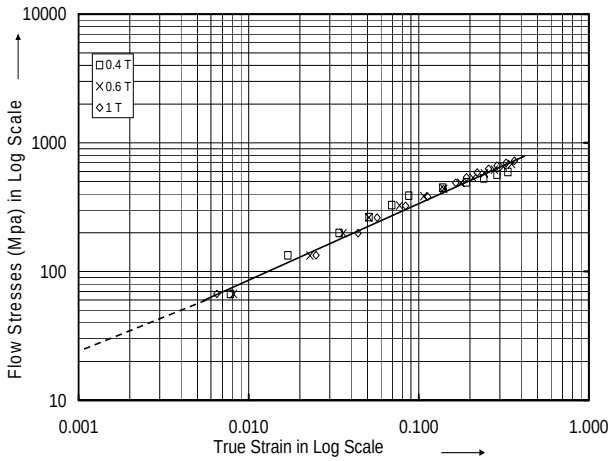

Fig. 1 Log-log plot between σ_z and ε_z

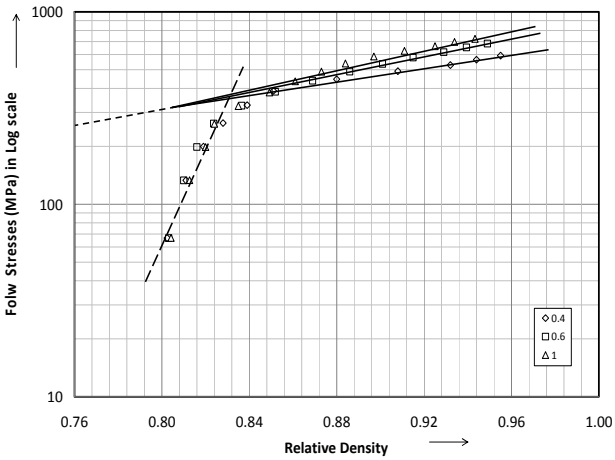

Fig. 2 Semi-log plot between σ_z and R

The general observation of Figs. 1 & 2 reveal that increase of strain and density increases its flow stresses, however the influence of aspect ratio is different in both the cases. In fact flow stress against strain, aspect ratios influence is practically negligible and is following single mechanism throughout. While flow stress against density follows two different mechanisms, accordingly the initial one is from 80% to 83% density that can be avoided for all practical purposes, as it is less span of density enhancement. In the later stage that is after around 83% density, aspect ratio influence is evident. *This reveals that higher the aspect ratio greater the flow stress for a given density, this is acceptable as the mass fraction of particle is higher for higher volume material, thus exhibits higher stress for the same density level*. Although, the nature of characteristics can be revealed from Fig. 1 & 2, for flow stress against strain and density that may not exhibit the true picture of strain hardening characteristics; as the material had undergone an incremental step of plastic deformation. Therefore using Eq. 5, 6 and Eq. 7, 8 instantaneous strength coefficient and hardening exponent for strain and density can be been calculated respectively. Accordingly Figs. 3 & 4 are plotted for K_i against strain and density respectively, Figs. 5 & 6 plotted for n_i against strain and density respectively. A similar plot for C_i and b_i are constructed and shown in Figs. 7 through 10 respectively.

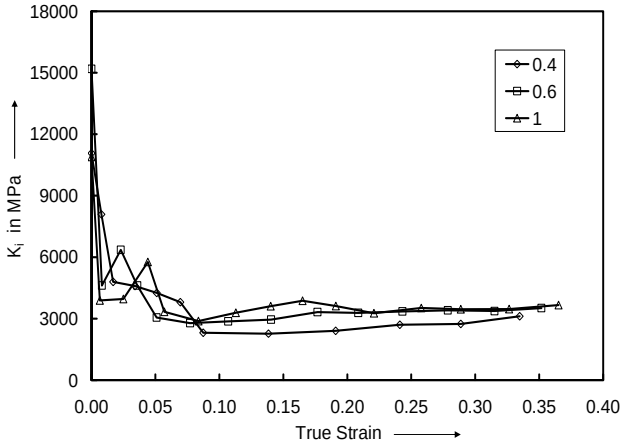

Fig. 3 Relationship between K_i and ε_z

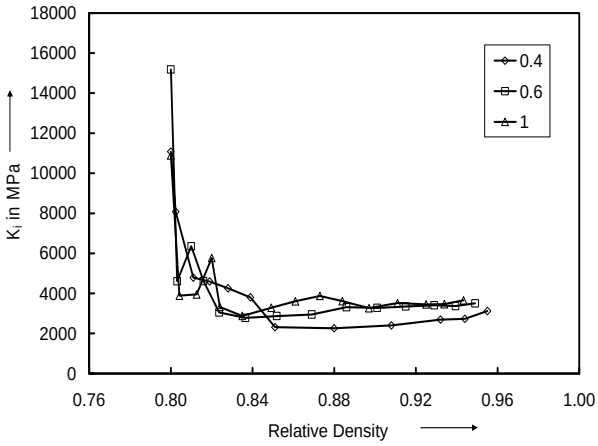

Fig. 4 Relationship between K_i and R

As seen in Figs. 3 & 4, the K_i values initially at peak and a sudden fall followed by a steady and mild enhancement, this behavior is true invariably for all the aspect ratios as well as for the parameters considered such as strain and density. Further close observation reveals that higher aspect ratios possess relatively higher strength coefficient comparing to its counterpart, however aspect ratio 1 and 0.6 practically shows nil difference. Although it's obvious that higher the volume

possess higher the strength, but at strain to fracture, the K_i values are in close proximity irrespective of aspect ratios. Almost similar observations can be noticed in referring to Figs. 5 & 6, but a steady enhancement in hardening exponent is clearly evident. The points in Figs. 5 & 6 are little fluctuated at initial stage is due to inhomogeneous deformation as the preforms are deformed under nil lubricant condition.

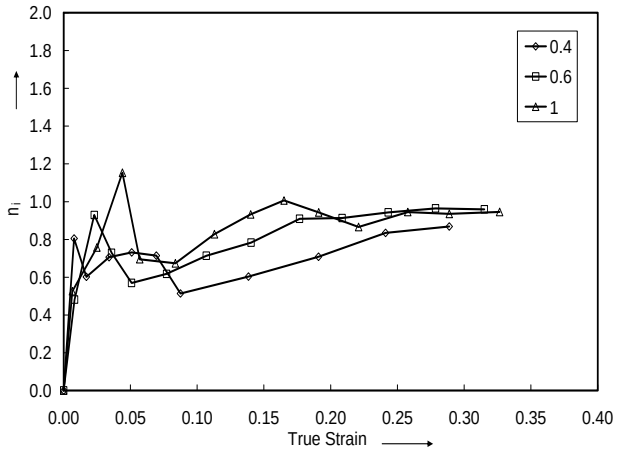

Fig. 5 Relationship between n_i and ε_z

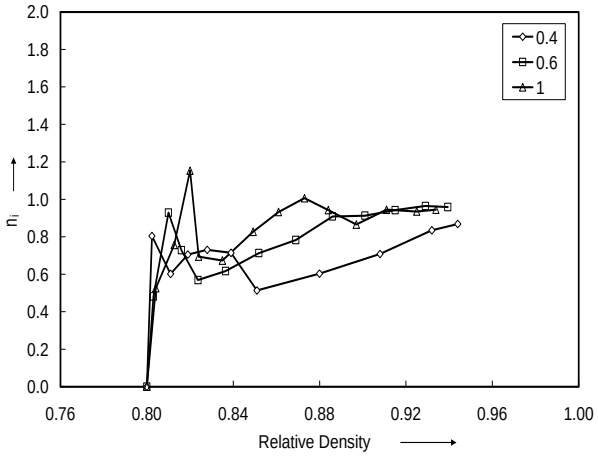

Fig. 6 Relationship between n_i and R

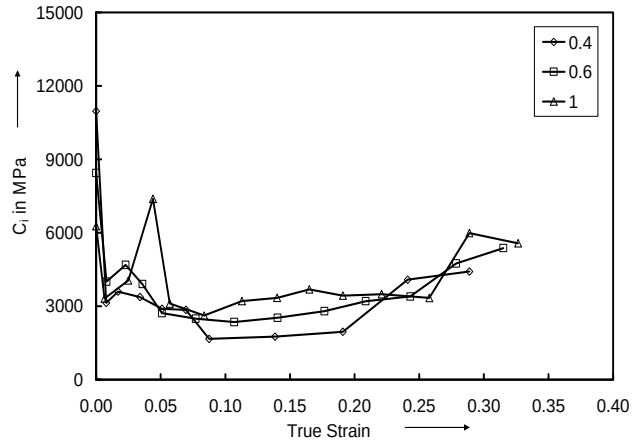

Fig. 7 Relationship between C_i and ε_z

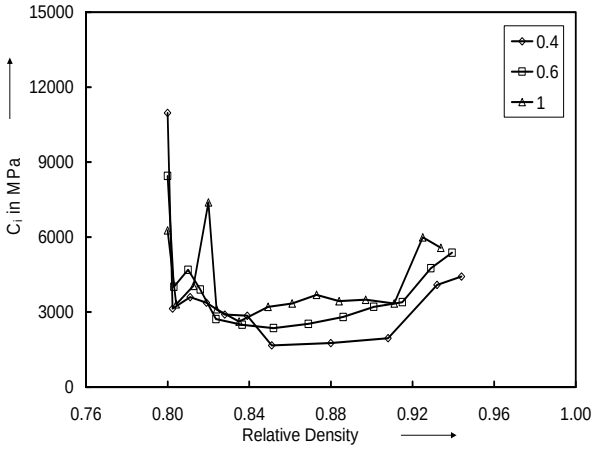

Fig. 8 Relationship between C_i and R

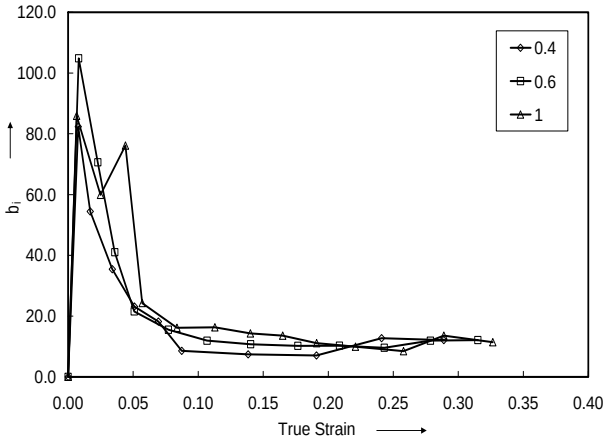

Fig. 9 Relationship between b_i and ε_z

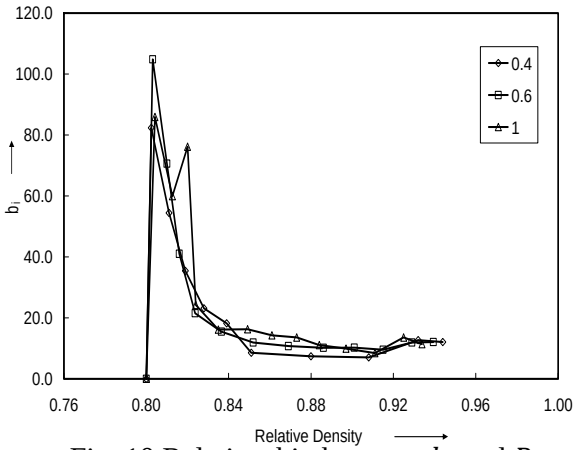

Fig. 10 Relationship between b_i and R

It is interesting to observe a similar characteristic nature from Figs. 7 through 10 as it was observed from Figs. 3 through 6. Therefore, *it is technically confirmed that density attainment is*

also an important process parameter that influences the mechanical strengthening of P/M preforms. Further an interesting and important phenomenon established by various researchers [3,6,9,11] are that P/M preforms undergo both geometric and matrix hardening under cold plastic deformation, comparing to a conventional material that experiences only matrix hardening. In this investigation, this can be rationalized by observing to the Figs. 3, 5, 7 & 9 exposes the matrix hardening, whilst Figs. 4, 6, 8 & 10 reveals the geometric hardening and so the constants K_i & n_i and C_i & b_i are the representative of the respective hardening mechanism. Meaning thereby, geometric hardening is due to closure of pores and so the effective volume decreases with constant mass, whilst matrix hardening is due to piling up of grains and grain boundaries during plastic deformation that greatly hinders the movement of dislocation that subsequently enhanced the resistance to deformation.

Conclusions

The higher aspect ratio preforms relatively possess higher strength coefficient and hardening exponent against induced strain and attained density comparing to its counterpart, however aspect ratios of 0.6 and 1 shows negligible influence in general. Closure of pores under plastic deformation enhanced the geometric work-hardening that was established by forming an empirical relationship between flow stress and density as, $\sigma = Ce^{bR}$. This equation is utilized to calculate and establish the instantaneous hardening behavior due to density. A very similar approach was carried out for establishing matrix work-hardening behavior between flow stress and strain. Finally, it can be concluded that invariable to aspect ratios, preforms experience work hardening due to strain as well as density.

References

[1] CC. Huang, JH. Cheng, An investigation into the forming limits of sintered porous materials under different operational conditions, J. Mater Process Technol. 148 (2004) 382-393.

[2] XQ. Zhang, YH. Peng, MQ, Li, SC. Wu, XY. Ruan, Study of workability limits of porous materials under different upsetting conditions by compressible rigid plastic finite element method. J Mater Eng Perform. 9 (2000)164-169.

[3] A. Rajeshkannan, S. Narayan, Strain hardening behaviour in sintered Fe-0.8%C-1.0%Si-0.8%Cu powder metallurgy preform during cold upsetting. J Engg Manufact. 223 (2009) 1567-1574.

[4] R M. German, Powder metallurgy science, second ed., Metal Powder Industries Federation, New Jersey, 1994, Ch: Full density processing, 301-338.

[5] MA. Taha, NA. El-Mahallawy, AM. El-Sabbagh, Some experimental data on workability of aluminium-particulate-reinforced metal matrix composites, J Mater Process Technol 202 (2008) 380-385.

[6] R. Narayanasamy, V. Anandakrishnan, KS. Pandey, Effect of geometric work-hardening and matrix work-hardening on workability and densification of aluminium-3.5% alumina composite during cold upsetting, Mater Des. 29 (2008) 1582-1599.

[7] DR. Kumar, C. Loganathan, R. Narayanasamy, Effect of glass in aluminum matrix on workability and strain hardening behavior of powder metallurgy composite, Mater Des 32 (2011) 2413-2422.

[8] K. Baskaran, R. Narayanasamy, An experimental investigation on work hardening behaviour of elliptical shaped billets of aluminium during cold upsetting, Mater Des. 29 (2008) 1240-1265.

[9] R. Ebrahimi, N. Pardis, Determination of strain hardening exponent using double compression test, Mater Sci Engg A. 518 (2009) 56-60.

[10] Dr. Kumar, R. Narayanasamy, C. Loganathan, Effect of glass and SiC in aluminum matrix on workability and strain hardening behavior of powder metallurgy hybrid composites. Mater Des 34 (2012) 120-136.

[11] A. Rajeshkannan, KS. Pandey, S. Shanmugam, R. Narayanasamy, Sintered eutectoid P/M steel behavior during cold upsetting, Materials Research, 11 (2008) 11-20.